Electronic Supplementary Material (ESI) for Journal of Materials Chemistry B.

Supporting information

Ultrafine Transition Metal Dichalcogenides Nanodots Prepared by Polyvinylpyrrolidone -assisted Liquid Phase Exfoliation

Shan Zhang,[ab] Jing Li*[a] and Erkang Wang*[a]

a. State Key Laboratory of Electroanalytical Chemistry, Changchun Institute of Applied Chemistry, Chinese Academy of Sciences, Changchun, Jilin, 130022, P. R. China. E-mail: ekwang@ciac.ac.cn; Tel: +86-431-85262003

b. University of Science and Technology of China, Hefei, Anhui, 230029, P. R. China.

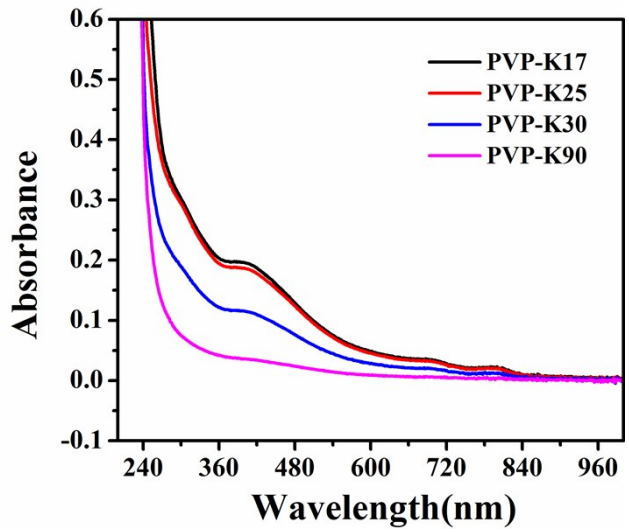

Figure S1. UV-vis spectra of $MoSe_2$-PVP dispersions exfoliated by PVP of different average molecular weight.

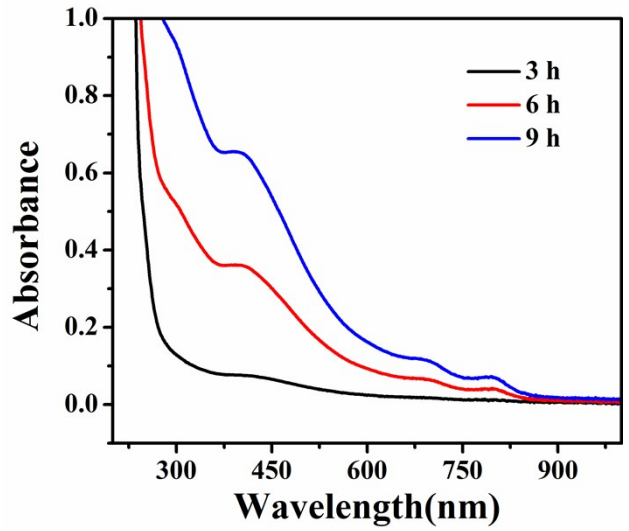

Figure S2. UV-vis spectra of $MoSe_2$-PVP dispersions in the presence of PVP-K17 obtained by different sonication time.

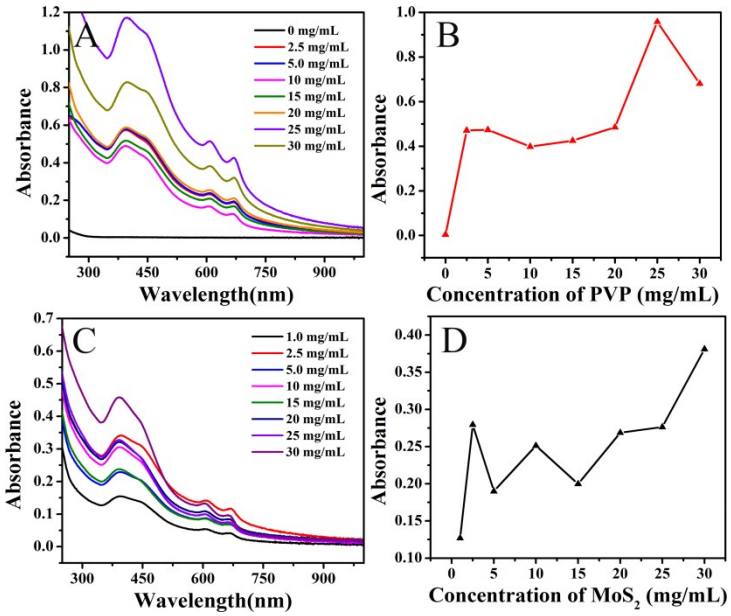

Figure S3. UV-vis absorption spectra of (A) certain amount of MoS_2 (2.5 mg/mL) obtained by sonication in various concentrations of PVP-K17, and (C) different concentrations of MoS_2 dispersions in the presence of certain amount of PVP-K17 (25 mg/mL). The tendency between UV-vis absorption of MoS_2-PVP dispersions located at 345 nm and various concentrations of PVP-K17 (B) and initial MoS_2 powder (D).

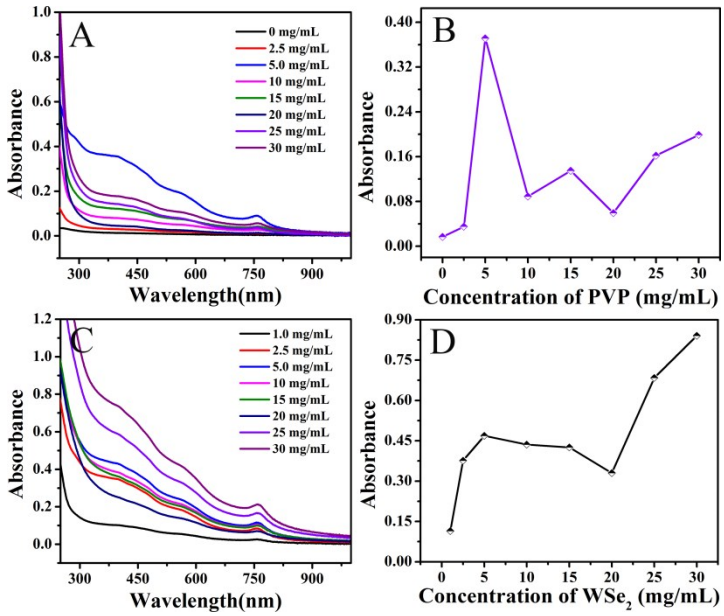

Figure S4. UV-vis absorption spectra of (A) certain amount of WSe_2 (2.5 mg/mL) obtained by sonication in various concentrations of PVP-K17, and (C) different concentrations of WSe_2 dispersion in the presence of certain amount of PVP-K17 (5 mg/mL). The tendency between UV-vis absorption of WSe_2-PVP dispersions located at 335 nm and various concentrations of PVP-K17 (B) and initial WSe_2 powder (D).

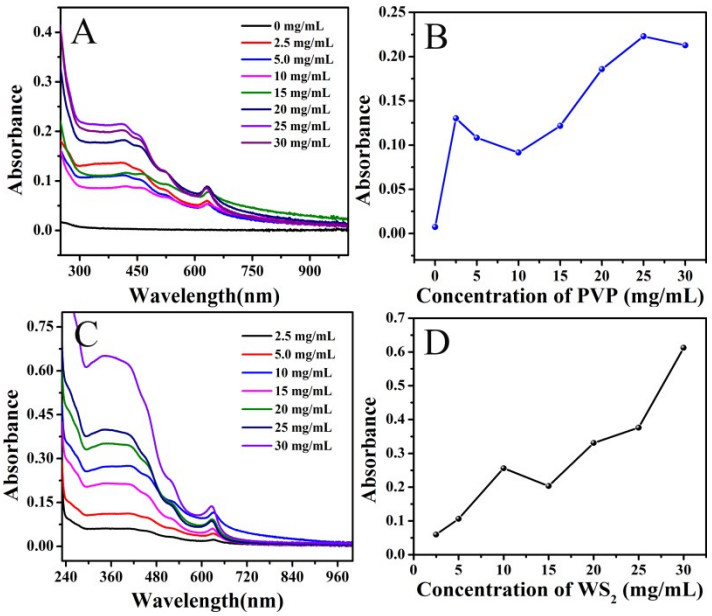

Figure S5. UV-vis absorption spectra of (A) certain amount of WS_2 (2.5 mg/mL) obtained by sonication in various concentrations of PVP-K17, and (C) different concentrations of WS_2 dispersion in the presence of certain amount of PVP-K17 (25 mg/mL). The tendency between UV-vis absorption of WS_2-PVP dispersions located at 295 nm and various concentrations of PVP-K17 (B) and initial WS_2 powder (D).

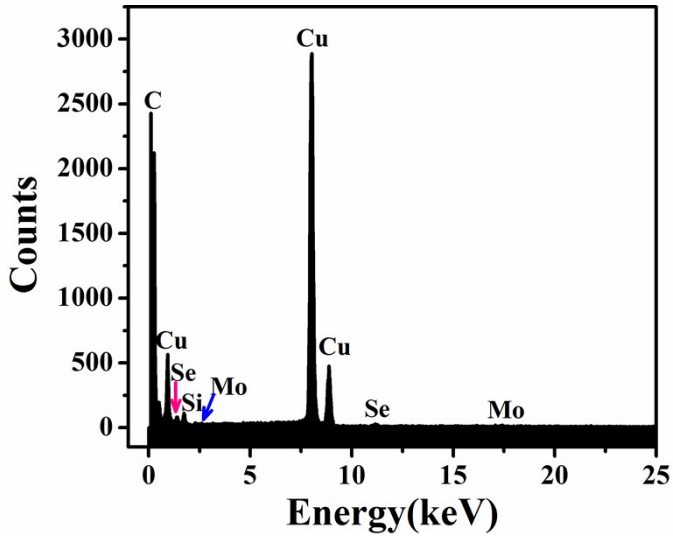

Figure S6. TEM-EDX pattern of $MoSe_2$-PVP nanocomposites.

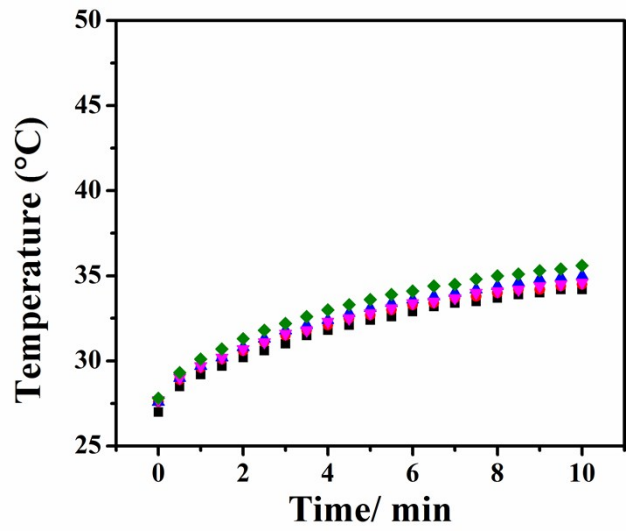

Figure S7. Photothermal heating curve of pure PVP-K17 with the same concentration as that in Figure 6A in the main text.

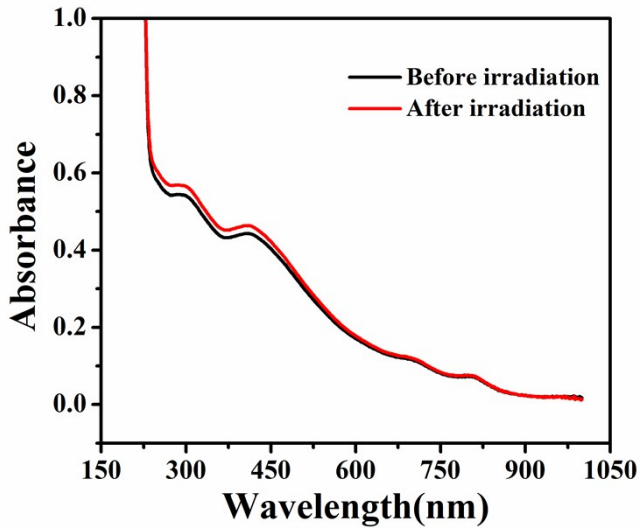

Figure S8. UV-vis spectra of $MoSe_2$-PVP dispersion (100 μg/mL) before and after 808 nm laser irradiation for successive six cycles with an on-and-off laser irradiation.

Table S1. Summary of the optimal concentrations of PVP-K17 and bulk crystal.

	Concentration of PVP (mg/mL)	Concentration of bulk crystal (mg/mL)
$MoSe_2$	20	15
MoS_2	25	2.5
WSe_2	5	5
WS_2	25	10